AIAA JOURNAL
Vol. 35, No. 2, February 1997

Influence of Elastomeric Damper Modeling on the Dynamic Response of Helicopter Rotors

Donald L. Kunz*
McDonnell Douglas Helicopter Company, Mesa, Arizona 85205

Several modeling approaches that describe the behavior of elastomeric materials used in helicopter rotor lag dampers are examined and evaluated, using laboratory test data. Two of the models are then used in a simulation of a helicopter rotor startup, and the simulation results are compared to one another and to flight test data. The models created using laboratory test results show that the simple, complex modulus model will yield good predictions of damper energy dissipation, but the simulation results indicate that this model is inadequate for predicting forced response. Although some of the models evaluated performed better than the others, none were free from limitations that would make them unsuitable for some applications. It is recommended that more effort be put into acquiring and analyzing damper test data to facilitate the development of more robust modeling approaches.

Nomenclature

a, b, c	= complex modulus exponential curve-fit coefficients ($a + bu^c$)
a_1, a_3, a_5	= Fourier cosine coefficients [Eq. (1)]
b_1, b_3	= Fourier sine coefficients [Eq. (1)]
C	= damping function, N ⋅cm^{-1} ⋅s^{-1}
c	= Voigt–Kelvin solid damping coefficient, N ⋅cm^{-1} ⋅s^{-1}
c_p	= anelastic displacement fields (ADF) solid damping, N ⋅cm^{-1} ⋅s^{-1}
c_0, c_2	= nonlinear Voigt–Kelvin solid damping coefficients, N ⋅cm^{-1} ⋅s^{-1}
f	= damper force, N
f_0	= initial damper force at $t = 0$, N
K	= stiffness function, N/cm
$K\prime$	= stiffness modulus, N/cm
$K\prime\prime$	= damping modulus, N/cm
k	= Voigt–Kelvin solid stiffness coefficient, N/cm
k_p, k_s	= ADF solid stiffnesses, N/cm
k_0, k_2, k_4	= nonlinear Voigt–Kelvin solid stiffness coefficients, N/cm
p_1, p_2, p_3	= stiffness modulus coefficients, N/cm
q_1, q_2, q_3	= damping modulus coefficients, N/cm
t	= time, s
u	= displacement, cm
v	= velocity, cm/s
W_{diss}	= damping energy, J
ω	= frequency, rad/s
$\bar{(\ )}$	= constant value
$\dot{(\ )}$	= derivative with respect to time

Introduction

ELASTOMERIC materials are used in a variety of parts on modern helicopters. Bearingless rotor helicopters, such as the McDonnell Douglas Explorer, the Bell Model 680, the Boeing/Sikorsky RAH-66, and the MBB BO-108, employ an elastomeric snubber-damper that serves both to restrain the motion of the pitch housing and to provide necessary lag damping to the rotor system. Elastomers are also used in the lag dampers of aircraft such as the McDonnell Douglas AH-64 Apache, the Bell Model 412, and the Boeing Model 360. Because of the fact that the use of elastomers in critical components of rotorcraft is now so widespread, the subject of elastomeric damper modeling has received increased attention in recent years.

For many years, the preferred method of describing the stiffness and damping properties of elastomers has been the complex modulus method. This method models the damper as a linear spring and a linear damper operating in parallel. However, it is clear from even the most rudimentary study of elastomeric material properties that linear modeling of elastomeric damper response is entirely inadequate. An in-depth discussion of the influence of the nonlinear characteristics of elastomers on the design of lag dampers is presented elsewhere.[1] That paper discusses the dependence of elastomeric material properties on factors such as amplitude and frequency of motion, temperature, and preload. However, instead of focusing on the effect of these factors on damper response characteristics, the emphasis is placed on how each factor affects the values of the linear complex moduli. It is clear that the investigation was tailored to focus on specific design parameters (e.g., spring rate and energy dissipation), rather than on developing a comprehensive damper model.

To keep the basic structure of the complex modulus method intact, modifications have been proposed that account for dual-frequency excitation[2] and thermal effects.[3] Felker et al.[2] propose that the damper force may be expressed as a spring force that is a nonlinear function of displacement, plus a damping force that is a nonlinear function of both displacement and velocity. Based on this nonlinear function, nonlinear complex moduli can be derived that are in much better agreement with measured moduli over a range of amplitudes. Starting with amplitude-dependent complex moduli, Hausmann and Gergely[3] examine the effect of heat buildup and environmental conditions on damper efficiency. In addition, they touch on the effects of amplitude and frequency variations, as well as polyharmonic loading.

Others make a break with the complex modulus approach. Gandhi and Chopra[4] place an additional nonlinear spring in series with the linear, parallel spring and dashpot. The rationale for representing the series spring by a quadratic function of the displacement is solely to improve the fidelity of the static response. However, it does nothing to account for nonlinear damping. The nonlinear model[5] is based on using the current and local peak velocities of a nonlinear damper. It is shown to correlate well with experimental data taken using sinusoidal excitation with both single and dual frequencies.

Other researchers[6,7] take a different approach to modeling elastomeric materials but arrive at nearly the same model as that proposed by Gandhi and Chopra.[4] This approach is based on the method of anelastic displacement fields (ADF), which is extended to model strain-dependent material behavior. The mechanical analogy of this model is structurally identical to that of Gandhi and Chopra,[4] except that now both springs and the dashpot are represented by nonlinear functions.

Received May 24, 1996; revision received Oct. 19, 1996; accepted for publication Oct. 22, 1996; also published in *AIAA Journal on Disc*, Volume 2, Number 2.

*R&E Specialist; currently Associate Professor, Department of Aerospace Engineering, Old Dominion University, Norfolk, VA 23529-0247. Associate Fellow AIAA.

In all of the investigations cited above, and in many others, improved elastomeric material models that have been applied to helicopter rotors have been evaluated on the basis of their effect on aeroelastic stability. Because energy dissipation is an integrated function of damper response, it is possible to derive a damper model that has the same total damping, but radically different response characteristics. Furthermore, aeroelastic stability is calculated from a set of equations that are linearized about an equilibrium state, effectively removing nonlinearities from the damper model during the stability computation. Therefore, it would appear that a representative damper model must provide a good approximation to the force-displacement characteristics of the damper, as well as duplication of its energy dissipation.

In this paper, the AH-64A elastomeric lag damper is used to investigate the relative merits of several modeling techniques. First, harmonic response data that were obtained from the Apache damper in laboratory bench tests is examined and characterized. Then, several different strategies that have been proposed for modeling elastomeric materials are examined and evaluated, using the data from those dampers. Finally, two of the damper models are integrated into a multibody analysis of the Apache blade assembly, and evaluated on the basis of how well they perform when compared to flight test measurements of transient blade motions.

Apache Lag Damper

In the Apache rotor system (Fig. 1), the lag dampers are attached, two per blade, between the pitch housing and the lead-lag link. The leading-edge and trailing-edge dampers are mounted identically with a trunnion connecting the inboard end of the damper to the pitch housing, and a rod end connecting the outboard end to the lead-lag link. As the blade undergoes lead-lag motion, the rotation of the lead-lag link imposes equal and opposite linear displacements on the leading-edge and trailing-edge dampers. These displacements are resisted by the force resulting from the shearing of the elastomeric material in the dampers.

The dampers used on the Apache are manufactured by Lord Corp., using an elastomer known as BTR VI. Four damper specimens were bench-tested by Lord to obtain typical values for the complex moduli ($K\prime$ and $K\prime\prime$). Each was subjected to a single, harmonic excitation at 2.42 Hz and the resultant force was measured. The stiffness modulus $K\prime$ is defined as the force component (per unit amplitude) that is in phase with the applied motion, and the damping modulus $K\prime\prime$ is defined as the force component (per unit amplitude) that is 90 deg out of phase with the applied motion. Figure 2 shows the measured properties as well as curve fits through those data. The curve fits were obtained using the exponential function, $a + bu^c$ (Table 1), which was selected after attempting fits using a variety of functional forms. This functional form, compared to polynomial fits for example, appears to provide a reasonable approximation to the data over the full range of interest.

In addition to the bench testing that produced the complex modulus data described above, forced-response testing was performed

Table 1 Complex modulus curve fits

$a + bu^c$	a	b	c
$K\prime$	7979	4453	−0.524
$K\prime\prime$	4277	1793	−0.644

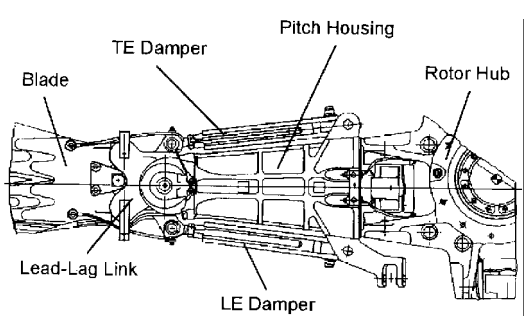

Fig. 1 Apache rotor hub configuration.

Table 2 Typical lag damper harmonic coefficients

Amplitude, cm	a_1	a_3	a_5	b_1	b_3
0.099	4,911	361	224	−3,552	−402
0.508	20,667	2,921	1,124	−9,970	−1,965

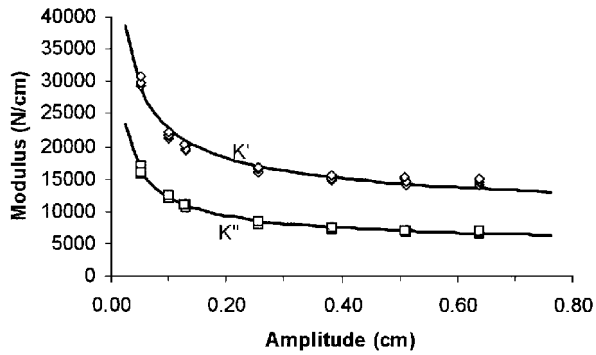

Fig. 2 Typical Apache lag damper properties: □ and ◇, measured properties and ——, curve fits.

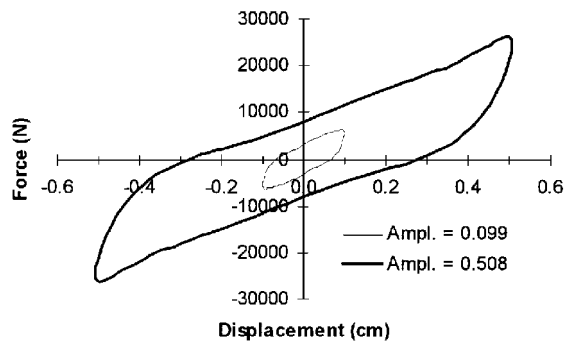

Fig. 3 Typical lag damper harmonic responses.

on the bench with nine lag dampers. These dampers were subjected to 2.42-Hz harmonic excitations at amplitudes of both 0.099 and 0.508 cm. Ten harmonics of the damper forces were recorded. Analysis of the bench-test data showed that only the first three odd cosine and first two odd sine components contributed significantly to the damper response function. Based on these data, a function that describes the damper force resulting from sinusoidal excitation at a single frequency can be written in the form

$$f = a_1\cos(\omega t) + a_3\cos(3\omega t) + a_5\cos(5\omega t) + b_1\sin(\omega t) + b_3\sin(3\omega t) \quad (1)$$

Figure 3 displays the force-displacement curves for typical harmonic damper response, based on the average of the nine dampers tested. The averaged harmonic components are tabulated in Table 2. It is obvious from both Figs. 2 and 3 that nonlinearities play a significant role in the forced response of the Apache lag damper. These data are used in the remainder of the paper as a basis for creating and evaluating various lag damper models.

It is instructive to observe the changes in the force-displacement curves that result from selectively eliminating higher harmonics of the damper response function. Figure 4 shows the changes in shapes of the force-displacement curves (0.508-cm excitation) when selected harmonic terms are removed from the response function [Eq. (1)]. When only the first harmonic terms are used in the response function (dashed line), the curve exhibits the classic oval shape of the complex modulus representation. Of course, the constants $K\prime$ and $K\prime\prime$ are defined as the first harmonic cosine and sine components of the response, so this result is to be expected. The addition of the third harmonic terms (dotted line) introduces the distinctive upturned and downturned points at the displacement extremes, and decreases the magnitude of the force produced as the displacement passes through zero. The addition of the fifth harmonic term (solid line) tends to

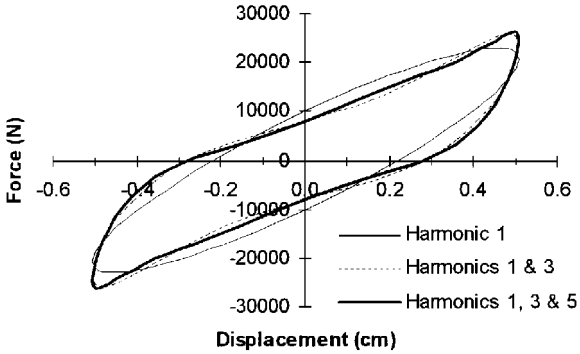

Fig. 4 Lag damper response harmonics.

enhance the features introduced by the third harmonic, sharpening the points at the large displacements, and making the curve nearly linear as it passes through zero displacement.

More interesting, however, is the effect that removing harmonics has on the energy dissipation,[1] as measured by

$$W_{\text{diss}} = \oint f \frac{\partial u}{\partial t}\,\mathrm{d}t \tag{2}$$

When Eq. (2) is applied to each of the force-displacement curves in Fig. 4, the resulting values of energy dissipation are identical. This is a significant observation, because it implies that the higher harmonic terms, which are responsible for the nonlinear response characteristics of the damper, have no impact on the energy dissipation characteristics of the damper. The obvious implication of this observation is that although the constants, $K\prime$ and $K\prime\prime$, which are used to define the complex modulus model, are sufficient to define the energy dissipation characteristics of elastomeric materials, they are not sufficient to describe the forced-response characteristics.

Lag Damper Models

Voigt–Kelvin Solid

Traditionally, elastomeric damper properties have been represented using the complex modulus method, which is equivalent to a linear Voigt–Kelvin solid (VKS). The mechanical analogy to a VKS[8] is shown in Fig. 5. In this approach, the values of the spring stiffness and the dashpot damping are often assumed to be constant. However, anyone who has observed the response of an elastomeric device to virtually any type of excitation would agree that this simple model is not an adequate representation of the elastomer.

The differential equation describing a nonlinear VKS (Fig. 5) can be written in the form

$$f = K(u)u + C(\dot{u}, u)\dot{u} \tag{3}$$

Linear Damper Properties

If the stiffness and damping in Eq. (3) are assumed to be constant values, the VKS model becomes equivalent to the traditional complex modulus representation. If the experimental data from Table 2 are used to define the values of k and c, the response to harmonic excitation is identical to the dashed line in Fig. 4, which includes only the first harmonic response.

Table 3 shows the closed-form solutions of Eq. (3) under different loading conditions, when k and c are assumed to be constants. Note that for constant force, constant displacement rate, and harmonic displacement, the form of the response function allows both of the constants k and c to be determined from a single test. In addition, steady-state measurements of the response to the constant displacement rate and harmonic displacement loading conditions can be used to determine both constants.

Nonlinear Damper Properties

To account for the nonlinear response characteristics of elastomeric materials, it has been proposed that the nonlinear properties of $K\prime$ and $K\prime\prime$ be used to define nonlinear stiffness and damping functions. For example, the definitions of $K\prime$ and $K\prime\prime$ from Table 1

Table 3 Closed-form solutions for a linear VKS

Load	Response
$f = \bar{f}$	$u = (\bar{f}/k)\{1 - \exp[(k/c)t]\}$
$u = \bar{u}$	$f = k\bar{u}$
$u = \bar{v}t$	$f = \bar{v}(c + kt)$
$u = \bar{u}\sin\omega t$	$f = \bar{u}(k\sin\omega t + c\omega\cos\omega t)$

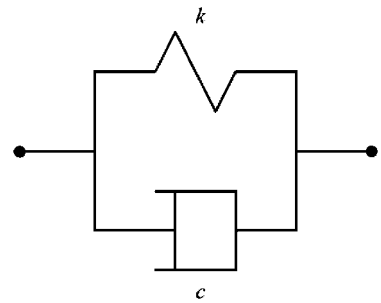

Fig. 5 Mechanical analogy to a VKS.

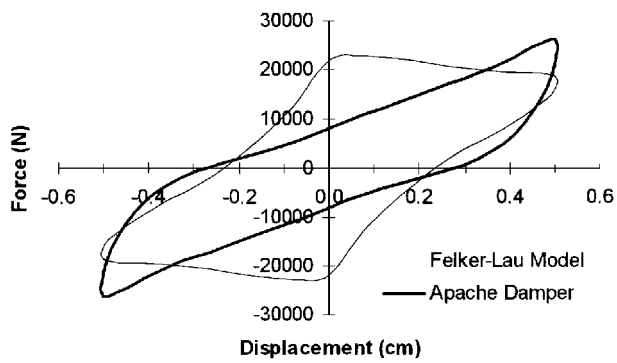

Fig. 6 Felker–Lau damper response (amplitude = 0.508 cm).

can be substituted (with a slight modification) into Eq. (3), resulting in the following expression for the damper force:

$$f = (7979 + 4453|u|^{-0.524})u + (4277 + 1739|u|^{-0.644})(\dot{u}/\omega) \tag{4}$$

The problem with using this expression for the damper force is that as u approaches zero, the value of f approaches infinity; and when $u = 0$, f is undefined. Therefore, the definitions from Table 1, although providing an excellent approximation to the $K\prime$ and $K\prime\prime$ measurements, are completely unacceptable for predicting damper response.

Felker et al.[2] present an alternative formulation, where the functions used to provide an approximation to $K\prime$ and $K\prime\prime$ are

$$\begin{aligned} K\prime &= p_0 + p_1|u| + p_2u^2 + \ldots \\ K\prime\prime &= q_0 + q_1|u| + q_2u^2 + \ldots \end{aligned} \tag{5}$$

A least-squares fit, applied to the data shown in Fig. 2, was used to determine the values of the constants in Eqs. (5). If Eqs. (5) are converted to stiffness and damping, then substituted into Eq. (3), the following expression for damper force results:

$$\begin{aligned} f = {} & (30{,}254 - 71{,}525|u| + 76{,}599u^2 + \ldots)u \\ & + (17{,}010 - 43{,}618|u| + 44{,}666u^2 + \ldots)(\dot{u}/\omega) \end{aligned} \tag{6}$$

Although Eqs. (5) do not provide as good an approximation to $K\prime$ and $K\prime\prime$ for the complete range of amplitudes, Eq. (6) has no singularity at zero displacement. However, as shown in Fig. 6, Eq. (6) grossly overpredicts the force near zero displacement, and consequently overpredicts the amount of energy dissipated by 36%. To be fair, Eq. (6) predictions fare much better for small-amplitude motion. For example, at an amplitude of 0.099 cm, the energy dissipation is overpredicted by less than 10%.

The fundamental problem with using the curves for K_I and K_{II} vs amplitude as a basis for deriving nonlinear stiffness and damping functions is that the response always will be dominated by the behavior of the functions near zero displacement. As shown in Fig. 2, both K_I and K_{II} measurements show a nearly exponential increase as the amplitude approaches zero. Therefore, any function that approximates those measurements must exhibit similar characteristics, and the resulting damper force will predict disproportionately high forces as the displacement goes through zero.

Nonlinear Forcing

Instead of basing the nonlinear stiffness and damping functions on the values of K_I and K_{II}, an alternative approach to modeling nonlinear dampers is to derive those functions from the nonlinear forced response. From bench testing of the damper, it is known that the damper force has the functional form shown in Eq. (1), for an imposed harmonic displacement of $u = \bar{u}\cos(\omega t)$. To express the damper force in terms of u and $\dot{u}$, and retain the same harmonic content as in Eq. (1), the stiffness and damping functions can be expressed in the form

$$k(u) = k_0 + k_2u^2 + k_4u^4 \qquad c(\dot{u}) = c_0 + c_2\dot{u}^2 \tag{7}$$

Substituting into Eq. (3), the equation for damper force then becomes

$$f = (k_0 + k_2u^2 + k_4u^4)u + (c_0 + c_2\dot{u}^2)\dot{u} \tag{8}$$

The stiffness and damping coefficients in Eqs. (7) now may be derived exactly in terms of the harmonic coefficients from Eq. (1):

$$k_0 = \frac{a_1 - 3a_3 + 5a_5}{\bar{u}} \qquad k_2 = \frac{4(a_3 - 5a_5)}{\bar{u}^3} \qquad k_4 = \frac{16a_5}{\bar{u}^5}$$
$$c_0 = \frac{-(b_1 + 3b_3)}{\omega\bar{u}} \qquad c_2 = \frac{4b_3}{(\omega\bar{u})^3} \tag{9}$$

Using the values of the harmonic coefficients from Table 2, and substituting into Eqs. (9), Eq. (8) becomes

$$f_{0.099} = [49970 - (3.126 \times 10^6)u^2 + (3.767 \times 10^8)u^4]u + (3160 - 471\dot{u}^2)\dot{u}$$
$$f_{0.508} = [34502 - (8.241 \times 10^4)u^2 + (5.317 \times 10^5)u^4]u + (2054 - 17\dot{u}^2)\dot{u} \tag{10}$$

Although this approach yields an exact equation for the harmonic damper force, it is exact only for a particular amplitude and frequency. By comparing Eqs. (10), it is easy to see that the stiffness and damping coefficients are dependent on amplitude. It may be possible to curve fit the coefficients in Eqs. (7) for a range of displacements and frequencies, but a much larger database of response data will be required as compared to that presented in Table 2.

ADF Solid

If one were to take the mechanical analogy to a VKS (Fig. 4) and add another spring in series, the result would be as shown in Fig. 7. The model described by Gandhi and Chopra uses this mechanical analogy, and assumes that only k_s is nonlinear. Govindswamy et al.,[6] starting with the theory of ADF, arrives at the same mechanical

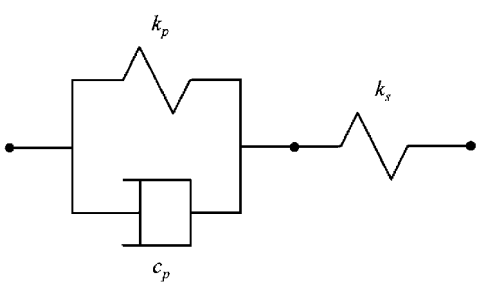

Fig. 7 Mechanical analogy to an ADF solid.

Table 4 Closed-form solutions for linear ADF model

Loading	Response
$f = \bar{f}$	$u = (\bar{f}/k_1) + (\bar{f}/k_2)\{1 - \exp[-(k_1/c_1)t]\}$
$u = \bar{u}$	$f = \frac{k_1k_2}{k_1 + k_2}\bar{u} + \left(f_0 - \frac{k_1k_2}{k_1 + k_2}\bar{u}\right)\exp\left(-\frac{k_1 + k_2}{c_1}t\right)$
$u = \bar{v}t$	$f = \frac{k_2}{k_1 + k_2}\left\{\frac{k_2}{k_1 + k_2}\left[1 - \exp\left(-\frac{k_1 + k_2}{c_1}t\right)\right] + \frac{k_1}{c_1}t\right\}c_1\bar{v}$
$u = \bar{u}\sin\omega t$	$f = \frac{k_2\bar{u}}{c_1^2\omega^2 + (k_1 + k_2)^2}\left\{[c_1^2\omega^2 + k_1(k_1 + k_2)]\sin\omega t + c_1k_2\omega\left[\cos\omega t - \exp\left(-\frac{k_1 + k_2}{c_1}t\right)\right]\right\}$

analogy but allows both springs and the damper to be nonlinear. The differential equation that describes the fully nonlinear ADF solid is

$$k_s^2c_p\dot{f} + (k_s^2 + k_s\dot{f})(k_p + k_s)f = k_s(k_s^2 + k_s\dot{f})(c_p\dot{u} + k_pu) \tag{11}$$

where k_p, k_s, and c_p may all be nonlinear functions of displacement and velocity.

Some insight into the characteristics of the ADF solid can be gained by looking at the closed-form solutions of this equation under different loading conditions, when k_p, k_s, and c_p are constants.

The first item worthy of note is that while the responses in Table 4 show significant differences from those in Table 3 (VKS), there are also some strong similarities. For example, the only difference in the responses to a constant force is that the stiffness expression in the ADF model is simply the equivalent stiffness for two springs in series. The same equivalent stiffness is apparent in the constant term of the ADF response to a constant displacement, but the corresponding VKS response has no exponential term.

Like the VKS, it is possible to calculate the stiffness and damping constants from the constant displacement rate and harmonic displacement loading conditions. However, unlike the VKS, it is not possible to determine all of the constants using only steady-state measurements of a single loading condition. For example, analysis of the steady-state response to harmonic displacement would produce sine and cosine components, but there are three constants that need to be determined for the ADF solid. Therefore, the determination of the stiffness and damping constants from steady-state data requires the use of more than one loading condition. In attempting to create a curve-fit ADF model of the data shown in Table 2, it was discovered that no acceptable fit could be obtained. Once it was realized that simple harmonic response data allows the determination of only two of the constants, the reason for the failure of the fitting process was understood.

For a linear model of the mechanical analogy in Fig. 7, one could determine the three constants by analyzing both the transient and steady-state responses to either the constant displacement rate or harmonic forcing. However, judging from the forms of the responses in Table 4, calculating the three constants would require solving nonlinear equations in the constants. On the other hand, a mathematically simpler solution would be to apply a constant force to the specimen until it was displaced a predetermined amount. Then, the displacement would be held constant until steady state was reached. The equivalent series stiffness could be calculated easily from the steady-state measurement, and curve fits to the transient sections of the displacement and force responses could be made. The solution for the stiffness and damping constants then only requires the solution of simple, linear equations. Naturally, such a procedure is subject to the availability of suitable test equipment. In addition, for a complete characterization of the material, a range of forces and displacements would have to be tested.

To create an approximate, nonlinear, ADF model from laboratory data, a similar procedure to that described above could be used. However, because the solutions in Table 4 are for a linear model, the procedure would carry the implicit assumption that the nonlinearities are small. Referring back to the data in Table 2, such an assumption would seem reasonable. Thus, instead of determining the values of constants from the steady-state and transient data, one

would determine the coefficients of the functional forms, and then solve for the function forms of the stiffnesses and damping.

Apache Blade Simulation

In this section, results from simulations using two different representations of the force-displacement equations for damper response are compared to flight test data. A fully nonlinear, geometrically exact model of the AH-64A Apache main rotor blade assembly was created for performing these simulations using the general-purpose, multibody system analysis program ADAMS. The model consists of 20 parts, representing the rotor hub, swashplate, pitch link, pitch housing, strap pack, leading- and trailing-edge lag dampers, lead-lag link, and blade. Except for the strap pack, all of the components are assumed to be rigid. Standard joints, primitive joints, and motion constraints are used to connect the parts to one another and maintain the geometry of the model. Elastic components, such as the feathering bearing, strap pack, and the lag dampers, are modeled by forces acting between parts. In one of the simulations, each damper is modeled as a linear VKS. The stiffness and damping are, therefore, constant values that are derived from the first-harmonic response alone. The other simulation models the dampers as nonlinear VKS, where the stiffness and damping functions are derived from Eqs. (7).

The flight condition used to compare damper models is a brake-on/release rotor startup. In the simulation, the rotor brake is initially locked, while the engines are spooled up. Then the brake is released, and the rotor is allowed to turn. The simulation starts when the brake is released. A smoothed torque profile (Fig. 8), derived from the flight-test measurements, is used to define the torque that is applied to the rotor shaft of the ADAMS model. The torque spike that is present at the beginning of the simulation is due to the sudden torque applied by the engines to the rotor shaft when the rotor brake is released. For a brake-off startup, this spike is not present. The torque spike induces a large lag response by the blade, and the prediction of this response poses a severe challenge to the simulation software. The ability to predict the lag response for the brake-on/release startup condition is important for two practical reasons: first, the lag response has a significant effect on the loads in other parts of the Apache blade retention system, and second, the damper design must be sufficiently stiff that the blade is not allowed to attain such a large lag angle that the lag stops are contacted. To select appropriate damper constants for the simulation, the maximum damper deflection was determined from the flight-test data. For this flight condition, the maximum lag angle was estimated to be 0.039 rad, which, when multiplied by perpendicular distance to the line of action of the lag damper, results in a damper deflection of approximately 0.45 cm. Therefore, the damper constants derived from the bench tests that applied a harmonic amplitude of 0.508 cm to the damper were used in this simulation.

The rotor speed predicted by the ADAMS simulations is compared to the measured rotor speed in Fig. 9. Because rotor speed can be expressed as an integral of the torque, multiplied by a constant that is proportional to the blade inertia, the rotor speed correlation is a good measure of the fidelity of the inertia properties of the model. The rotor speed predicted using both the linear and nonlinear damper model tracks the measured speed exceptionally well for the entire

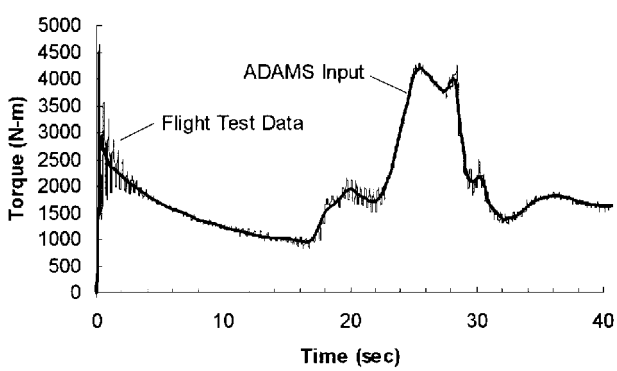

Fig. 8 Rotor torque input.

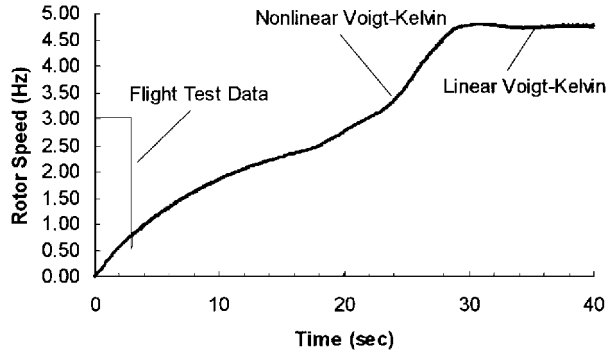

Fig. 9 Correlation of rotor speed predictions.

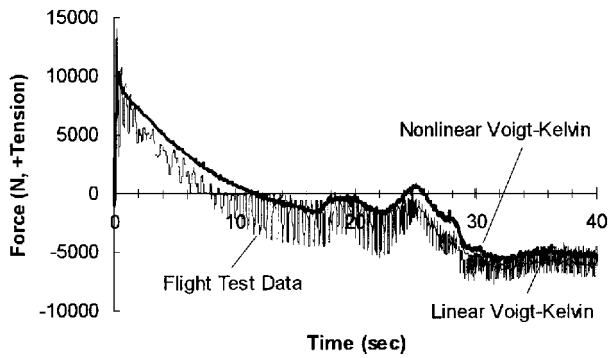

Fig. 10 Correlation of leading-edge lag damper predictions.

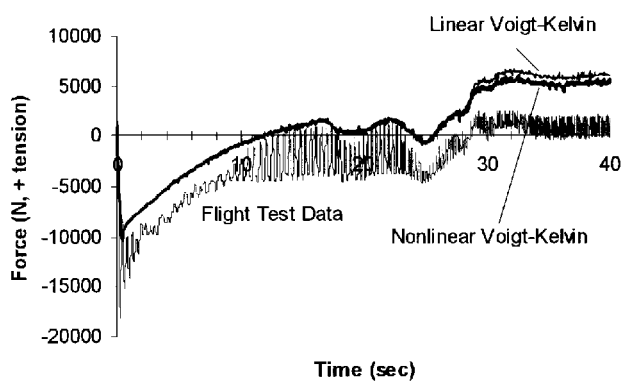

Fig. 11 Correlation of trailing-edge lag damper predictions.

40 s of the simulation. Note that a simple drag function, which is proportional to the square of the rotor speed and an average value of the profile drag of the HH-02 airfoil, is used to keep the rotor speed from running away. The accuracy of the rotor speed predictions is therefore somewhat dependent on the choice of the profile drag coefficient, particularly in the latter stages of the simulation when the rotor speed is large. However, on the basis of the correlation shown in Fig. 9, this model appears to have excellent fidelity in predicting the inertial loads on the blade.

Figures 10 and 11 show the damper force in the leading-edge and trailing-edge dampers, respectively, as compared to damper force measurements. The forces predicted by both the linear and the nonlinear models are consistently 1500–2000 N greater than the test data for the first 25 s of the simulation. One explanation that proposes to account for this difference is that there is a preload on the aircraft dampers that the model does not include. However, checks of the assembly drawings and conversations with flight-test mechanics indicate that there is no preload applied to the dampers during installation. Another possible explanation is that measurement error in the load cells accounts for the offset. Although this is certainly possible, it is unlikely that the load cells on both dampers would be erroneously offset by the same amount.

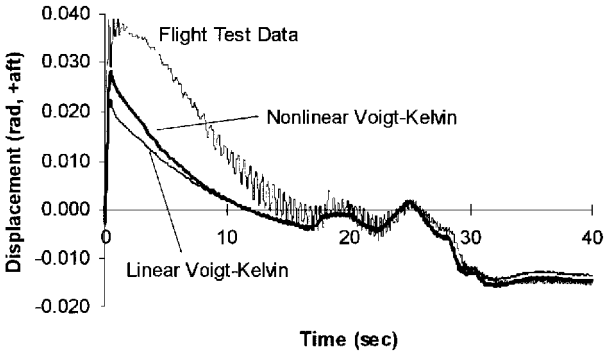

Fig. 12 Correlation of lag angle predictions.

The most likely explanation of the difference between the flight-test data and the simulation is based on the fact that after several hours of operation, the dampers have been observed to acquire a permanent set. If it is assumed that the dampers acquire a set with the blades lagging, the simulation would be expected to consistently overpredict the damper forces. Note also that after 25 s, the predictions of leading-edge damper force track much closer to the test data than do the predictions of trailing-edge damper force. Although there is no explanation available for this observation, the damper force predictions remain symmetric and the measured loads are nonsymmetric.

Of greatest interest in the context of this paper is the comparison of the predicted and measured lag angles in Fig. 12. For the linear damper model, immediately after the brake is released, the maximum predicted lag angle reaches approximately 55% of the maximum measured lag angle. However, it does manage to catch up with the measurements 20 s into the simulation and tracks quite well from then on. The nonlinear model performs better than the linear model immediately after brake release but still falls nearly 30% short of the measurements. It also catches up to the measurements after about 20 s. The results of this simulation show that neither the linear nor the nonlinear model is capable of accurately predicting the response of the blade under a large impulsive load.

Conclusions and Recommendations

Based on comparisons of the various lag damper models and on the results of the dynamics simulations, the following conclusions can be made:

1) The linear complex modulus approach to modeling the behavior of elastomeric dampers will produce accurate estimates of energy dissipation, but it is not sufficient for prediction of forced response.

2) Modifications to the complex modulus method that derive nonlinear damper properties from the nonlinear $K\prime$ and $K\prime\prime$ properties cannot be expected to give accurate estimates of energy dissipation and are not suitable for prediction of forced response.

3) Damper modeling using the nonlinear VKS method (based on response measurements) will result in accurate estimates of energy dissipation and is suitable for the prediction of forced response. However, this methodology is limited in that the damper models are amplitude-dependent

4) The ADF approach appears to be an attractive, and more general, alternative to the VKS. However, because there is an additional parameter (or function) to be identified, additional data over and above that required to identify the VKS parameters are required.

5) Simulation of a brake-on/release rotor startup is a rigorous test of the lag damper model. Although the simulations presented herein demonstrated generally good correlation with flight-test data, the weaknesses of the damper models could be identified readily. Clearly, simulations of this type are more suitable for evaluating models of elastomeric dampers than are calculations of aeroelastic stability.

Some of the damper models performed quite well, but all were saddled with severe restrictions. To remove some of these restrictions and to permit more robust damper models, the following recommendations are made:

1) More data must be generated in controlled environments to perform detailed studies of the influence of amplitude and frequency on harmonic response, and displacement and velocity on nonharmonic response. In addition, the data should be structured so as to facilitate comparisons of the relationship between harmonic and nonharmonic response.

2) The testing methods used for characterization of elastomeric materials need to be reexamined. Clearly, response to simple harmonic forcing using a single frequency and two amplitudes is insufficient to fully describe the material characteristics. In addition, the traditional parameters $K\prime$ and $K\prime\prime$ are inadequate for any model more sophisticated than the linear complex modulus model, and need to be augmented with additional parameters.

3) Elastomeric lag damper models that are developed in the future should be evaluated against realistic data that possess a strong nonharmonic content and provide a rigorous test of the model's capabilities.

References

[1]Hausmann, G., "Structural Analysis and Design Considerations of Elastomeric Dampers with Viscoelastic Material Behavior," Twelfth European Rotorcraft Forum, Paper 70, Garmisch-Partenkirchen, Germany, Sept. 1986.

[2]Felker, F. F., Lau, B. H., McLaughlin, S., and Johnson, W., "Nonlinear Behavior of an Elastomeric Lag Damper Undergoing Dual-Frequency Motion and Its Effect on Rotor Dynamics," *Journal of the American Helicopter Society*, Vol. 32, No. 4, 1987, pp. 45–53.

[3]Hausmann, G., and Gergely, P., "Approximate Methods for Thermoviscoelastic Characterization and Analysis of Elastomeric Lead-Lag Dampers," Eighteenth European Rotorcraft Forum, Paper 88, Avignon, France, Sept. 1992.

[4]Gandhi, F., and Chopra, I., "An Analytical Model for a Nonlinear Elastomeric Lag Damper and Its Effect on Aeromechanical Stability in Hover," American Helicopter Society Aeromechanics Specialists Conf., San Francisco, CA, Jan. 1994.

[5]Tarzanin, F. J., and Panda, B., "Development and Application of Nonlinear Elastomeric and Hydraulic Lag Damper Models," *AIAA/ASME/ASCE/AHS/ASC 36th Structures, Structural Dynamics, and Materials Conference* (New Orleans, LA), AIAA, Washington, DC, 1995 (AIAA Paper 95-1449).

[6]Govindswamy, K., Lesieutre, G. A., Smith, E. C., and Beale, M. R., "Modeling Strain-Dependent Dynamic Behavior of Viscoelastic Structures Using Anelastic Displacement Fields," *AIAA/ASME/ASCE/AHS/ASC 36th Structures, Structural Dynamics, and Materials Conference* (New Orleans, LA), AIAA, Washington, DC, 1995 (AIAA Paper 95-1403).

[7]Smith, E. C., Beale, M. R., Govindswamy, K., Vascsinec, M. J., and Lesieutre, G. A., "Formulation, Validation, and Application of a Finite Element Model for Elastomeric Lag Dampers," 51st Annual Forum of the American Helicopter Society, Fort Worth, TX, May 1995.

[8]Popov, E. P., "Linearly Viscoelastic Materials," *Introduction to Mechanics of Solids*, Prentice–Hall, Englewood Cliffs, NJ, 1968, pp. 116–123.